



Cancelling teleportation error in legacy IMC code for photonics (without tilts, with simple minimal modifications)

Gaël Poëtte, Xavier Valentin, Adrien Bernede

► To cite this version:

Gaël Poëtte, Xavier Valentin, Adrien Bernede. Cancelling teleportation error in legacy IMC code for photonics (without tilts, with simple minimal modifications). Journal of Computational and Theoretical Transport, 2020. hal-02530492v2

HAL Id: hal-02530492

<https://hal.science/hal-02530492v2>

Submitted on 16 May 2020

HAL is a multi-disciplinary open access archive for the deposit and dissemination of scientific research documents, whether they are published or not. The documents may come from teaching and research institutions in France or abroad, or from public or private research centers.

L'archive ouverte pluridisciplinaire **HAL**, est destinée au dépôt et à la diffusion de documents scientifiques de niveau recherche, publiés ou non, émanant des établissements d'enseignement et de recherche français ou étrangers, des laboratoires publics ou privés.

Cancelling teleportation error in legacy IMC code for photonics (without tilts, with simple minimal modifications)

Gaël Poëtte^a, Xavier Valentin^b, Adrien Bernede^b

^a*CEA DAM CESTA, F-33114 Le Barp, France*

^b*CEA DAM DIF, F-91297 Arpajon, France*

Abstract

Monte-Carlo (MC) schemes for photonics have been intensively studied throughout the past decades, see [1] for a complete review. The recent ISMC scheme described in [2] presents many advantages (no teleportation error, converging behaviour with respect to the spatial and time discretisations). But it is rather different from the IMC one (it is based on a different linearisation and needs a slightly different code architecture). On another hand, legacy codes are often based on IMC implementations. For this reason, it remains important to be able to cancel the teleportation error within IMC codes. Cancelling the teleportation error within the IMC framework is also important for fair comparisons between both the IMC and the ISMC linearisations. This paper aims at suggesting some simple corrections to apply to an IMC implementation to completely cancel the teleportation error.

Keywords: Transport, Monte-Carlo, Numerical scheme, Photonics, IMC, ISMC

1. Introduction

Monte-Carlo (MC) schemes for photonics have been intensively studied throughout the past decades, see [3, 4, 5, 6, 7, 8, 9, 10, 11, 12] and the references in review paper [1]. From the seminal work of Fleck [3]¹, to the implicitation of the solver [4]², and some numerous corrections [12, 7, 9, 1]³, until the recent ISMC scheme [2]⁴, many consequential improvements have been made. The recent ISMC scheme described in [2] presents many advantages and is amongst the most efficient MC scheme for photonics. But it is rather different from the IMC one (it is based on a different linearisation and needs a slightly different code architecture). On another hand, legacy codes are often based on IMC implementations. For this reason, it remains important to be able to cancel the teleportation error within IMC codes. Cancelling the teleportation error within the IMC framework is also important for fair comparisons between both the IMC and the ISMC linearisations. This paper aims at suggesting some simple corrections to apply to an IMC implementation to obtain

Email addresses: gael.poette@cea.fr (Gaël Poëtte), xavier.valentin@cea.fr (Xavier Valentin), a.bernede@protonmail.com (Adrien Bernede)

¹whose linearisation demands unaffordable time steps.

²leading to affordable time steps but introducing the teleportation error.

³tilts of different order or different nature, on-the-fly resampling etc.

⁴by construction without teleportation error nor competing behavior between the spatial and time discretisations.

similar properties: completely cancelling the teleportation error and the competing behaviour of the spatial and time discretisation put forward in [7] and analysed in [2]. Care is also taken to compare both 'teleportation error free' MC schemes (the new IMC one of the present paper and ISMC) to highlight their respective strengths and weaknesses.

The paper is organised as follows: in section 2, we briefly present the system we are interested in together with the asymptotic limit we aim at capturing accurately (namely the equilibrium diffusion limit). In section 3, we present the IMC linearisation [4] on which many solvers (and also the original solver of this paper) are based. In section 4, we describe an original way to discretise, with an MC scheme, the IMC system. The new MC solver is not based on 'source sampling' hence does not foster any teleportation errors, see [2]. Care will be taken to highlight how an already implemented IMC solver can be easily corrected to cancel the teleportation error. The paper ends with benchmarks (in section 5) in which we verify numerically the aforementioned properties and put forward the fact that the new solver does not have some competing discretisation parameters. We also systematically compare the new IMC scheme to ISMC.

2. The system and its asymptotic limit of interest

In this article, we are interested in the Monte-Carlo (MC) resolution of the time-dependent, nonlinear, radiative transfer equations. The model has general form (see [13]):

$$\begin{cases} \frac{1}{c} \partial_t I + \omega \cdot \nabla I + \sigma_t I = \sigma_a B(T_m) + \sigma_s \int_{4\pi} I \frac{d\omega'}{4\pi}, \\ \partial_t E(T_m) = \int_{4\pi} c \sigma_a \left(\frac{I}{4\pi} - B(T_m) \right) d\omega'. \end{cases} \quad (1)$$

In the above equations, $I = I(t, x, \omega)$ and $T_m(t, x)$ are the unknowns of the system and stand respectively for the intensity of radiation energy and the material temperature. Variables $t \geq 0$, $x \in \Omega \subset \mathbb{R}^3$ and $\omega \in \mathbb{S}^2$ are respectively the time, space and angle variables. The cross-sections $\sigma_t = \sigma_t(x, t)$, $\sigma_a = \sigma_a(x, t)$ and $\sigma_s = \sigma_s(x, t)$ are given functions of (x, t) . They stand for the total, absorption and scattering opacities. In particular, we have $\sigma_t = \sigma_a + \sigma_s$. The density of internal energy E depends on T_m via an equation of state $dE = \rho C_v(T_m) dT_m$ with ρ the mass density and C_v the heat capacity (constant for a perfect gas). The quantity $B(x, t) = a T_m^4(x, t)/4\pi$ is the frequency-integrated Planck function with a the radiative constant. The quantity c denotes the speed of light. In this paper, we are particularly interested in being able to accurately capture a particular regime: in diffusive media, system (1) behaves, at leading order, like the nonlinear diffusion equation on $\Phi_r(T_r) = a T_r^4 = \int_{4\pi} \frac{I}{4\pi} d\omega$

$$\begin{cases} \partial_t (\Phi_r(T_r) + E(T_r)) - \nabla \cdot \left(\frac{c}{3\sigma_t} \nabla (\Phi(T_r)) \right) = \mathcal{O}(\delta), \\ \Phi_r(T_r) = \int_{4\pi} \frac{I}{4\pi} d\omega = B(T_m) + \mathcal{O}(\delta). \end{cases} \quad (2)$$

With $\int_{4\pi} \frac{B(T_m)}{4\pi} d\omega = a T_m^4$ and $\Phi_r(T_r) = a T_r^4$, the second equation is equivalent to $T_m = T_r$: the radiative and matter temperatures are at equilibrium. In the above equation, $\delta \sim 0$ is a small parameter characterising what is commonly called the *equilibrium*⁵ *diffusion*⁶ limit [6, 7, 1].

⁵Equilibrium means $T_m = T_r$.

⁶Diffusion refers to the presence of the second order spatial term in (2).

The limit can be defined by introducing a characteristic length \mathcal{X} , a characteristic time \mathcal{T} and a characteristic collision rate λ and assuming we have

$$\begin{cases} \frac{c\mathcal{T}}{\mathcal{X}} = \mathcal{O}(\frac{1}{\delta}), \\ \frac{c\mathcal{T}}{\lambda} = \mathcal{O}(\frac{1}{\delta^2}), \end{cases} \quad (3)$$

with $\delta \sim 0$ small. System (1) and its limit (2) are relevant to model photons incoming into opaque media [13, 14, 15].

In this article, due to the high-dimensional problem we aim at tackling, we only focus on MC based numerical solvers.

The aim of this paper is to provide a new and original correction fitted to the IMC linearisation to cancel the teleportation error and the competing behaviours of the spatial and time discretisations (studied in [7, 2]). For this reason, we briefly describe IMC in the next section together with the drawbacks of having to resort to source sampling within the MC discretisation.

3. The Implicit Monte Carlo (IMC) method and the drawbacks of source sampling

Let us first describe the IMC (for Implicit Monte-Carlo) linearisation. IMC has been introduced in [4]. The idea is to introduce some sort of implicitness on B in the time discretization scheme in order to mitigate the effects of the stiff coupling between radiation and material. Implicit time discretization of (1) yields the following linear system:

$$\begin{cases} \frac{1}{c} \partial_t I + \omega \cdot \nabla I + \sigma_t^n I = \sigma_a^n B^{n+1} + \sigma_s^n \int_{4\pi} I \frac{d\omega'}{4\pi}, \\ \partial_t E = \int_{4\pi} c \sigma_a^n \left(\frac{I}{4\pi} - B^{n+1} \right) d\omega'. \end{cases} \quad (4)$$

To solve system (4) using an MC scheme, one has to provide an estimation of the source term $\sigma_a^n B^{n+1}$ which is unknown at the beginning of the time step. In [4], the authors propose a particular *estimation* of B^{n+1} that leads to the Fleck and Cummings equations that approximate the original system (1). We sum up the construction of B^{n+1} in the few next lines for the grey approximation. System (1) can be rewritten with respect to variables $(I, \Phi \equiv aT_m^4)$ instead of variables (I, T_m) :

$$\begin{cases} \frac{1}{c} \partial_t I + \omega \cdot \nabla I + \sigma_t I = \sigma_a \Phi + \sigma_s \int_{4\pi} I \frac{d\omega'}{4\pi}, \\ \partial_t \Phi = \int_{4\pi} c \sigma_a \beta(\Phi) \frac{I}{4\pi} d\omega - c \sigma_a \beta(\Phi) \Phi, \text{ with } \beta = \frac{d\Phi}{dE}. \end{cases} \quad (5)$$

Note that $\beta = \frac{d\Phi}{dE}$ has been introduced to express $\partial_t E$ with respect to $\partial_t \Phi$. In a sense, this term deals with all the physics relative to the equation of state (eos) $E(T_m) = E(T_m(\Phi))$ together with making sure the system can be closed using variables (I, Φ) .

The above system is still nonlinear. A linearisation is mandatory to apply an MC scheme. Integration of the radiation-material energy balance equation on time step $[t^n, t^{n+1}]$, using the backward Euler scheme for Φ and the forward Euler scheme for σ_a and β yields:

$$\Phi^{n+1} = \Phi^n + \int_{t^n}^{t^{n+1}} \int_{4\pi} c \sigma_a^n \beta^n \frac{I}{4\pi} d\omega - c \sigma_a^n \beta^n \Delta t \Phi^{n+1}. \quad (6)$$

The MC solver resulting from the above hypothesis is commonly called *implicit* but strictly speaking, it looks more like an *explicit-implicit*⁷ discretization of the second equation of (5). Still, in this paper, to remain consistent with the literature, we use the term *implicit* to describe the solver.

The above expression (6) can be easily inverted in term of Φ^{n+1} to give:

$$\Phi^{n+1} = f^n \Phi^n + (1 - f^n) \int_{t^n}^{t^{n+1}} \int_{4\pi} \frac{I}{4\pi} d\omega \frac{dt}{\Delta t}, \text{ with } f^n = \frac{1}{1 + c\sigma_a^n \beta^n \Delta t}.$$

The quantity f^n is the so-called Fleck factor. Replacing the time integral by its instantaneous value and using the approximation of Φ^{n+1} in the transport equation yields the time-discretized IMC system:

$$\begin{cases} \frac{1}{c} \partial_t I + \omega \cdot \nabla I + \sigma_t^n I = f^n \sigma_a^n \Phi^n + [\sigma_s^n + (1 - f^n) \sigma_a^n] \int_{4\pi} I \frac{d\omega'}{4\pi}, \\ \partial_t E = c f^n \sigma_a^n \left(\int_{4\pi} \frac{I}{4\pi} d\omega - \Phi^n \right). \end{cases} \quad (7a)$$

$$\quad (7b)$$

Notice that by redefining $\Sigma_a^n \leftarrow f^n \sigma_a^n$ and $\Sigma_s^n \leftarrow \sigma_s^n + (1 - f^n) \sigma_a^n$, $\Sigma_t^n = \sigma_t^n$ one obtains a transport equation similar to the first equation of (4) except that the emission term $S = f^n \sigma_a^n \Phi^n$ is now known because it is evaluated at the beginning of the time step. The time-discretized transport equation above has been supplemented by the proper material energy equation. Choosing to work on E instead of Φ here ensures, by construction, the conservation of the total energy for the system matter+photons provided Φ^{n+1} can be deduced from E^{n+1} (using the eos).

Equations (7) form a closed linear system on time step $[t^n, t^{n+1}]$. Obtaining a numerical approximation for equation (1) then consists in solving successively the two equations of system (7)

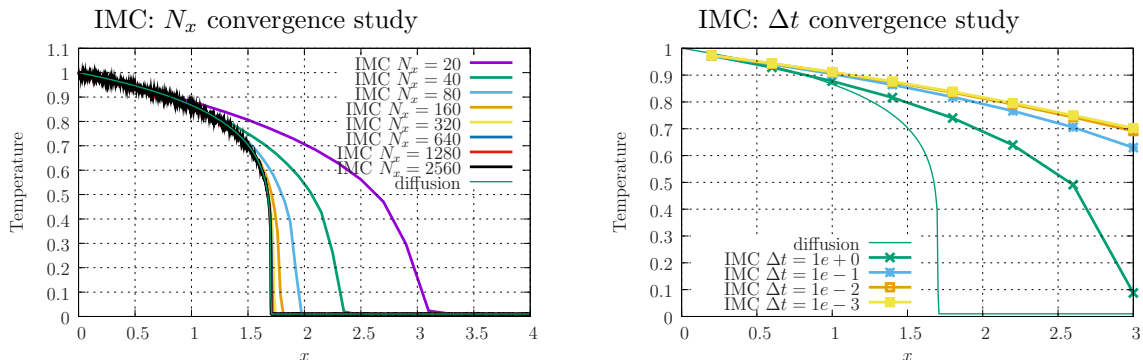


Figure 1: Convergence studies on the material temperature profiles $T(x, t^* = 500)$ at $t^* = 500$ for the IMC scheme, with respect to $N_x \in \{20, 40, 80, 160, 320, 640, 1280, 2560\}$ (left) and to $\Delta t \in \{10^0, 10^{-1}, 10^{-2}, 10^{-3}\}$ (right).

within every time step. During time step $[t^n, t^{n+1} = t^n + \Delta t]$,

- (*) the transport equation (7a) is solved with an MC method. The source term is classically treated with a *source sampling* strategy. Source sampling relies on the application of Duham-

⁷explicit with respect to σ, β , implicit with respect Φ .

mel's principle stating that if I_1 is solution of

$$\begin{cases} \frac{1}{c} \partial_t I_1 + \omega \cdot \nabla I_1 + \sigma_t^n I_1 = [\sigma_s^n + (1 - f^n) \sigma_a^n] \int_{4\pi} I_1 \frac{d\omega'}{4\pi}, \\ I_1(x, t = 0, \omega) = I(x, t = 0, \omega) = I_0(x, \omega), \end{cases} \quad (8)$$

and I_2 is solution of

$$\begin{cases} \frac{1}{c} \partial_t I_2 + \omega \cdot \nabla I_2 + \sigma_t^n I_2 = f^n \sigma_a^n \Phi^n + [\sigma_s^n + (1 - f^n) \sigma_a^n] \int_{4\pi} I_2 \frac{d\omega'}{4\pi}, \\ I_2(x, t = 0, \omega) = 0, \end{cases} \quad (9)$$

then $I_1 + I_2$ is solution of (7a). This implies one can track the already existing MC particles with an MC scheme (I_1) and sample 'source MC particles' (I_2) and track them independently to add them up, see [16].

- (**) The material energy E^{n+1} is updated solving (7b) by tallying the radiation energy deposit in the material with a *track length estimator* [17] during the MC resolution.

Basically, the problem comes from point (*) above and the use of source sampling to take into account the source term $S(x) = f^n \sigma_a^n \Phi^n(x)$, as detailed in [2]. In [2], the teleportation error occurring when a small spatial discrepancy δ_x within Φ^n is studied:

$$\Phi^n(x) = \Phi_{approx}^n(x) + \mathcal{O}(\delta_x^k).$$

In the above expression, k is the order of the spatial approximation of $x \rightarrow \Phi^n(x)$ within each cell. Typically, IMC as in [4] (i.e. no tilt) corresponds to taking $k = 1$ and constant approximations in each cell i , i.e. $\Phi_i^n(x) \equiv \Phi_i^n$. Tilted IMC, known to mitigate the teleportation error [12, 7, 1], corresponds to taking $k \geq 2$: a first order tilt ($k = 2$) consists in evaluating coefficients⁸ ($\Phi_{i,0}^n, \Phi_{i,1}^n$) and assuming that $\Phi^n(x)$, in cell i , is close to linear, i.e. $\Phi_i^n(x) \equiv \Phi_{i,0}^n + \Phi_{i,1}^n x$. Of course, more elaborated (second order, continuous etc.) tilts exist [12, 7, 9, 1], but they all suppose having a finite spatial accuracy, here denoted by $\mathcal{O}(\delta_x^k)$ with k the order of the approximation.

In the equilibrium diffusion limit, it has been shown in [2, 16] that, during time step $[t^n, t^{n+1}]$, as $N_{MC} \rightarrow \infty$, at leading order with respect to δ **and** δ_x in the equilibrium diffusion regime characterised by (3), system (7) behaves like (see [2, 16]):

$$\begin{cases} \partial_t \Phi_r - \nabla \left[\frac{c}{3\sigma_t^n} \nabla \Phi_r \right] + D_k \frac{\delta_x^k}{2\Delta t} \nabla^k \Phi_r = \mathcal{O} \left(\frac{\delta_x^{k+1}}{\Delta t} \right) + \mathcal{O}(\delta), \\ \partial_t E = \frac{1}{\beta^n \Delta t} [\Phi_r - \Phi^n] + \mathcal{O}(\delta) + \mathcal{O}(\delta_x^{k+1}). \end{cases} \quad (10)$$

From the comparison of (2) and (10), one can expect the numerical solution obtained from any MC scheme

- to exhibit isotropy for Φ_r (given enough MC particles),
- to recover the equilibrium property $\Phi_r = \Phi$ of (2) but only up to a Δt accuracy (i.e. $\Phi_r - \Phi^n = \mathcal{O}(\Delta t)$) once the IMC linearisation applied, see (10),
- but to exhibit a competing behaviour between Δt and δ_x :

⁸Usually, Φ_{approx}^n is based on a Taylor development and $\Phi_{i,1}^n$ is a first order spatial derivative.

- for a first order $\mathcal{O}(\delta_x^{k=1})$ approximation (corresponding to the original IMC solver of [4]) of Φ^n , a numerical advection term $D_1 \frac{\delta_x}{\Delta t} \nabla \Phi_r$ appears. The spatial discrepancy δ_x must be small with respect to the time step Δt to be able to recover a diffusive behaviour.
- for a second order $\mathcal{O}(\delta_x^{k=2})$ approximation of Φ^n (commonly called a *tilt* in the literature), an additional diffusive term $D_2 \frac{\delta_x^2}{\Delta t} \nabla^2 \Phi_r$ appears. In this case, the limit equation is a diffusion one but to recover the good diffusion coefficient ($\frac{c}{3\sigma_t^n}$), δ_x^2 must be small with respect to Δt .
- for a third order (and also for $k \geq 3$) reconstruction, the good diffusion coefficient is recovered but the competing behaviour remains, even if lessened by the fact δ_x is put to the power 3 (or more if $k+1 > 3$). Still, on coarse meshes, this may be problematic (see the examples given in [7, 2]).
- and to recover the diffusion coefficient $\frac{c}{3\sigma_t^n}$ provided a fine tuning between the spatial discretization and the time step as explained above and in [2].

Let us end this section with the results obtained with IMC and source sampling on a benchmark presented in [7]. A short description is provided in Appendix A. The aim of the next figures is to illustrate the previous points. Figure 1 presents two convergence studies: the first one is with respect to the spatial parameter $N_x = \{20, 40, 80, 160, 320, 640, 1280, 2560\}$ for $\Delta t = 5 \times 10^{-2}$ and $N_{MC} \approx 10^7$ on the left hand side and the second one is with respect to $\Delta t \in \{10^0, 10^{-1}, 10^{-2}, 10^{-3}\}$ for $N_x = 10$ (coarse mesh = important δ_x) and the same number of MC particles on the right hand side. The figure displays the material temperature at time $t^* = 500$ for the above meshes and time steps. The reference solution, obtained from a (finely resolved) deterministic solver for the equilibrium diffusion limit (2), is also plotted. With figure 1 (left), we recover the fact that for fixed Δt , the IMC solver converges toward the reference solution. But the convergence is slow. The finer the mesh, the noisier the results as we kept the number of MC particles N_{MC} almost constant (up to source sampling fluctuations). With this study, we emphasize the stakes of having a faster convergence with respect to N_x : less cells will be needed but also less MC particles, hence a potential important gain (see [2]). With figure 1 (right), we recover that for a fixed spatial discretization $N_x = 10$, the IMC results are worse and worse as Δt decreases. With this study, we briefly put forward the diverging behaviour (closely related to the δ_x discrepancy introduced by source sampling) of the scheme with respect to the time step for a fixed spatial discretization (more details are given in [2]).

Remark 3.1. *This diverging phenomenon when decreasing the time step for a fixed grid is what we call a competing behavior between the spatial and the time discretizations.*

Now, figure 2 presents the same convergence studies but with the ISMC scheme of [2]. For ISMC, the equilibrium diffusion limit during time step $[t^n, t^{n+1}]$, as $N_{MC} \rightarrow \infty$, at leading order with respect to δ , see [2], is given by

$$\begin{cases} \Phi_r = \Phi + \mathcal{O}(\Delta t) + \mathcal{O}(\delta), \\ \partial_t(E + \Phi_r) - \nabla \left[\frac{c}{3\sigma_t^n} \nabla \Phi_r \right] = \mathcal{O}(\delta), \end{cases} \quad (11)$$

It echoes (10) for IMC. From (11), we can see that ISMC does not suffer from any spatial discrepancy related to the grid, at least at first order with Δt and δ : it does not suffer the teleportation error

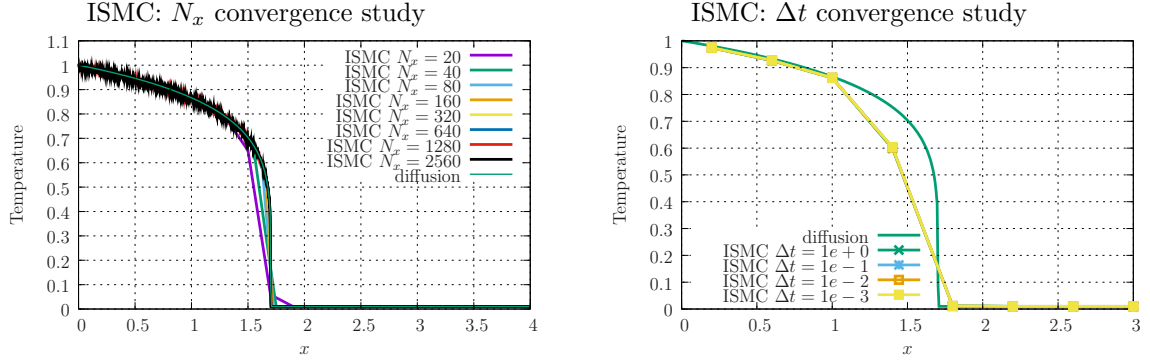


Figure 2: Convergence studies on the material temperature profiles $T(x, t^* = 500)$ at $t^* = 500$ for the ISMC scheme of [2], with respect to $N_x = \{20, 40, 80, 160, 320, 640, 1280, 2560\}$ (left) and to $\Delta t \in \{10^0, 10^{-1}, 10^{-2}, 10^{-3}\}$ (right).

on the diffusion equation. Furthermore, equilibrium is fulfilled provided a small enough time step. The ISMC solver (see left picture of figure 2) shows a fast spatial (N_x) convergence toward the reference solution. Furthermore, the results obtained with the ISMC solver (left picture of figure 2) tend to show that the new MC scheme is not sensitive (at least in a diverging way) to a decrease of Δt : every curves for $\Delta t \in \{10^0, 10^{-1}, 10^{-2}, 10^{-3}\}$ are indistinguishable. This benchmark confirms the new ISMC scheme has no teleportation error and allows avoiding the competing behaviour of Δt and δ_x .

The question now is: why describing a new MC scheme in this paper if ISMC provides the desired properties? The ISMC does have them but is based on a different linearisation leading to a different code architecture, see [2]. Many legacy codes are based on the IMC linearisation. The stakes of this paper are to be able to build an IMC solver without teleportation error and without a competitive behaviour between the spatial and time discretizations. We even aim at doing it with minimal modifications of an already existing IMC implementation. Once this is done, fair comparisons between the new IMC solver and the ISMC one of [2] can be done (see section 5 of this paper).

4. Avoiding source sampling for the MC discretization of the IMC linearisation

As explained in the previous section, regarding the teleportation error/slow spatial convergence rate and the competing behaviour of spatial and time discretisations, source sampling is incriminated (more details about this point are given in [2]). It is besides a parallel contention point, see [18]. In this section, we present a different way to take into account a source term. The idea is to make sure we have, by construction, $\delta_x = 0$ within the IMC linearisation.

Let us introduce a spatial grid of N_x non-overlapping cells such that the spatial domain $x \in \Omega \subset \mathbb{R}^3$ is tessellated into $\Omega = \Omega^{N_x} = \bigcup_{i=1}^{N_x} \Omega_i$. We rely on constant per cell discretisations of the opacities and source term. As a consequence, we assume we have access, at every beginning of time

steps $[t^n, t^n + \Delta t]$, to quantities

$$\begin{aligned}\sigma_\alpha^n(x) &\approx \sum_{i=1}^{N_x} \sigma_\alpha^{n,i} \mathbf{1}_{\Omega_i}(x), \forall \alpha \in \{s, t, a\}, \\ \psi^n(x) &\approx \sum_{i=1}^{N_x} \psi^{n,i} \mathbf{1}_{\Omega_i}(x), \forall \psi \in \{\beta, I, E, f\},\end{aligned}$$

with $\mathbf{1}_{\Omega_i}(x)$ denoting the indicatrix⁹ of cell Ω_i . In particular, we have

$$\begin{aligned}E^{n,i} &= \frac{1}{|\Omega_i|} \int_{\Omega_i} E(x, t^n) dx \text{ and } I^{n,i} = \frac{1}{|\Omega_i|} \int_{\Omega_i} \int_{4\pi} \frac{I(x, t^n, \omega)}{4\pi} dx d\omega, \\ \beta^{n,i} &\approx \beta(\Phi^{n,i}) \text{ and } f^{n,i} \approx f(\sigma_a^{n,i}, \beta^{n,i}).\end{aligned}$$

In other words, *all the above quantities are constant in each cell of the mesh*¹⁰. In the following paragraphs, we assume every above quantities are approximated on the N_x point grid even if not (abusively) reminded in the notations.

To describe the scheme, we first focus on equation (7a) which can be recast as

$$\partial_t I + c\omega \cdot \nabla I + c\Sigma_t I = S + c\Sigma_s \int_{4\pi} I \frac{d\omega'}{4\pi}, \quad (12)$$

with $\Sigma_t(x) = \sigma_t^n(x)$, $\Sigma_s(x) = \sigma_s^n(x) + (1 - f^n)\sigma_a^n(x)$ and $S(x) = cf^n(x)\sigma_a^n(x)\Phi^n(x)$ defined on the mesh Ω^{N_x} . The idea is to avoid having to resort to source sampling and take the source term into account *on-the-fly* during the MC resolution. For this, we suggest rewriting (12) as¹¹

$$\begin{aligned}\partial_t I + c\omega \cdot \nabla I + c\Sigma_t I &= S + c\Sigma_s \int_{4\pi} I \frac{d\omega'}{4\pi}, \\ &= \int_{4\pi} \frac{S}{4\pi} d\omega' + c\Sigma_s \int_{4\pi} I \frac{d\omega'}{4\pi}, \\ &= \int_{4\pi} \left(\frac{S}{I} + c\Sigma_s \right) I \frac{d\omega'}{4\pi}, \\ &= \int_{4\pi} (s(I) + c\Sigma_s) I \frac{d\omega'}{4\pi},\end{aligned} \quad (13)$$

where $s(x, I(x, t, \omega)) = \frac{S(x)}{I(x, t, \omega)}$ is a nonlinear term. As a consequence, we are going to need an additional linearisation hypothesis at this stage.

Remark 4.1. *This may represent a first drawback with respect to IMC (with source sampling) or ISMC.* With ISMC, an MC solver without source sampling can be built without additional hypothesis as soon as the time discretisation (and implicitation) is introduced, see [2].

⁹i.e. we have $\mathbf{1}_{\Omega_i}(x) = 1$ if $x \in \Omega_i$, $\mathbf{1}_{\Omega_i}(x) = 0$ if $x \notin \Omega_i$.

¹⁰i.e. no need for a tilt or any spatial reconstructions within the cells.

¹¹To go from the first to the second equation, the isotropy of the source term is used.

To suggest a relevant linearisation hypothesis here, we make an analogy between Quasi-Static methods, well-known and commonly applied for the linear Boltzmann equation coupled to the Bateman system (neutronics), see [19, 20, 21, 22, 23, 24]. Quasi-static methods are closely related to Asymptotic-Preserving schemes (see [16]) and suppose identifying a *relevant reduced model* before plugging it into (13). For this reduced model, we suggest the isotropic homogeneous one within each cell of Ω^{N_x} defined by

$$\begin{cases} \partial_t U^i(t) = S^i - c\Sigma_a^i U^i(t), \\ U^i(0) = U_0^i, \forall i \in \{1, \dots, N_x\}, \end{cases} \quad (14)$$

with $\Sigma_a^i = \Sigma_t^i - \Sigma_s^i \forall i \in \{1, \dots, N_x\}$. We insist (14) is solved within each cell $(\Omega_i)_{i \in \{1, \dots, N_x\}}$ in which constant per cell quantities are considered. Reduced model (14) has above all been chosen because

- it treats the source term,
- it can be solved analytically within each cell Ω_i and is consequently cheap to evaluate: its solution is given by

$$U^i(t) = \left(U_0^i e^{-c\Sigma_a^i t} + S^i \frac{1 - e^{-c\Sigma_a^i t}}{c\Sigma_a^i} \right). \quad (15)$$

We will assume (14) is valid per cell for all $x \in \Omega_i$ and along any characteristics $x + c\omega t \in \Omega_i$, $\forall i \in \{1, \dots, N_x\}$. With the above hypothesis, (13) becomes

$$\begin{aligned} \partial_t I + c\omega \cdot \nabla I + c\Sigma_t I &= \int_{4\pi} \left(\frac{S}{U} + c\Sigma_s \right) I \frac{d\omega'}{4\pi}, \\ &= c\Sigma_S \int_{4\pi} I \frac{d\omega'}{4\pi}, \end{aligned} \quad (16)$$

and is now linear. Above, we implicitly defined $c\Sigma_S = \frac{S}{U} + c\Sigma_s$. We will also intensively use the notation $\Sigma_A = \Sigma_t - \Sigma_S$.

It only remains to design an MC scheme to solve (16). An MC particle is defined by

$$i_p(x, t, \omega) = w_p(t) \delta_x(x_p(t)) \delta_\omega(\omega_p(t)), \quad (17)$$

where $w_p(t)$ is the weight of the MC particle, $x_p(t)$ its position and $\omega_p(t)$ its angle, every one of them at time t . Several MC schemes are at hand. Their descriptions come with the descriptions of the operations one must apply to $(w_p, x_p, \omega_p)_{p \in \{1, \dots, N_{MC}\}}$ to make sure every $(i_p)_{p \in \{1, \dots, N_{MC}\}}$ are solutions of (16). MC schemes intensively use the linearity of (16): if $\forall p \in \{1, \dots, N_{MC}\}$, i_p is of the form (17) and is solution of (16), then $\sum_{p=1}^{N_{MC}} i_p(x, t, \omega)$ is solution of (16) and approximates $I(x, t, \omega)$. In the following paragraphs, we describe briefly two converging (in law¹²) strategies (cf. theorem 3.2.1 of [17]) and justify our choice:

¹²Convergence *in law* is also commonly called *weak* convergence and is defined as such: a sequence of probability measures $(d\mu_n)_{n \in \mathbb{N}}$ is said to converge in law toward measure $d\mu$ if $\int f(x) d\mu_n(x)$ converges toward $\int f(x) d\mu(x)$ as n goes to infinity for all bounded Lipschitz function f . In our MC context, n echoes N_{MC} and $d\mu_n = \sum_{p=1}^n i_p(x, t, \omega)$ (the Dirac δ_x, δ_ω in (17) are measures with our notations).

- the *non-analog* MC scheme (see [24, 16]) requires that,
 - on any interval of time $[0, t]$ the particle position is updated according to $x_p(t) = x_p(0) + c\omega_p(0)t$.
 - The weight is modified along the flight path of each MC particle: on any interval of time $[0, t]$ such that the particle remains within cell Ω_i , the weight of the MC particle is multiplied by $w_p(t) = w_p(0)e^{-\int_0^t c\Sigma_A^i(\alpha)d\alpha}$. A few computations show that

$$w_p(t) = w_p(0)e^{-\int_0^t c\Sigma_A^i(\alpha)d\alpha} = w_p(0)\frac{U^i(t)}{U^i(0)} = w_p(0)\left(e^{-c\Sigma_a^i t} + S^i\frac{1 - e^{-c\Sigma_a^i t}}{c\Sigma_a^i U_0^i}\right). \quad (18)$$

This is equivalent to solving (14) along the flight path of each MC particle. If $S = 0$, we recover the classical weight modification $w_p(t) = w_p(0)e^{-c\Sigma_a^i t} = w_p(0)\frac{V^i(t)}{V^i(0)}$ solution of

$$\begin{cases} \partial_t V^i(t) = -c\Sigma_a^i V^i(t), \\ V^i(0) = V_0^i, \end{cases}$$

for the non-analog MC scheme without source term.

- Let τ denote a collision time: the MC tracking needs the sampling of a new scattering angle $\omega_p(\tau) = W$. In this paper, scattering being isotropic, the sampled angle W must be drawn from the uniform distribution on \mathbb{S}^2 and $\omega_p(\tau)$ is independent of $\omega_p(0)$. The reader interested on the construction of anisotropic scattering distributions can refer to [16].
- The sampling of the collision time τ within cell Ω_i must be made thanks to $\Sigma_S^i(t)$ from the probability measure

$$f_\tau(t) = c\Sigma_S^i(t)e^{-\int_0^t c\Sigma_S^i(\alpha)d\alpha}.$$

The interaction time τ can be sampled from an uniform law \mathcal{U} on $[0, 1]$ by inverting the cumulative density function associated¹³ to f_τ . This leads to (see [16, 24])

$$-\ln(\mathcal{U}) = \int_0^\tau c\Sigma_S^i(\alpha)d\alpha.$$

The integral on the right hand side can be computed exactly, but the inversion needed afterward is, to our knowledge, impossible to carry out analytically. A newton or an iterative method could be used (as in [24] for example) but we here aim at dealing with diffusive media (which would need many *on-the-fly* costly calls to the inversion algorithm). An approximation could be made (see remark 10.3 of [16]) but we here would like to avoid it as the MC scheme presented in this paper has already one more assumption than the ISMC solver of [2], see remark 4.1. For this reason, the **non-analog scheme is here discarded** despite its good property with respect to the weight modification.

- On another hand, the *semi-analog* MC scheme (see [16]) requires that

¹³Introduce F_τ the integral of f_τ , then by definition, see [25], $\tau = F_\tau^{-1}(\mathcal{U})$ where \mathcal{U} is uniformly distributed on $[0, 1]$.

- on any interval of time $[0, t]$ the particle position is updated according to $x_p(t) = x_p(0) + c\omega_p(0)t$.
- the weight of the MC particles remains unchanged if no collision occurs between times 0 and t so that $w_p(t) = w_p(0)$.
- Let τ denote a collision time:
 - the MC tracking needs the sampling of a new scattering angle $\omega_p(\tau)$ at the collision location $x(\tau) = x_p(0) + c\omega_p(0)\tau$ and collision time τ . Once again, scattering being isotropic, the sampled angle $\omega_p(t) = W$ must be drawn from the uniform distribution on \mathbb{S}^2 .
 - Furthermore, the weight of the MC particle encountering a collision within cell Ω_i must be multiplied by $w_p(\tau) = w_p(0) \frac{\Sigma_S^i(\tau)}{\Sigma_t^i(\tau)}$. As a consequence, for our problem of interest, the weight modification at the collision point is given by

$$\frac{\Sigma_S^i(\tau)}{\Sigma_t^i(\tau)} = \frac{\frac{S^i}{U^i(\tau)} + c\Sigma_s^i}{c\Sigma_t^i} = \frac{1}{c\Sigma_t^i} \left(\frac{S^i}{\left(U_0^i e^{-c\Sigma_a^i t} + S^i \frac{1 - e^{-c\Sigma_a^i t}}{c\Sigma_a^i} \right)} + c\Sigma_s^i \right), \quad (19)$$

and is analytical (no additional hypothesis required for efficiency). Note that once again, if $S = 0$, we recover the classical weight modification $\frac{\Sigma_s^i}{\Sigma_t^i}$ for the semi-analog MC scheme without source term.

- Finally, the sampling of the collision time within cell Ω_i must be made thanks to $\Sigma_t^i(t)$ from the probability measure

$$f_\tau(t) = c\Sigma_t^i(t) e^{-\int_0^t c\Sigma_t^i(\alpha) d\alpha}.$$

The interaction time τ can be sampled from an uniform law \mathcal{U} on $[0, 1]$ as

$$-\ln(\mathcal{U}) = \int_0^\tau c\Sigma_t^i(\alpha) d\alpha,$$

see [16, 24]. In our context, $\Sigma_t^i(t) = \Sigma_t^i = \sigma_t^{n,i}$ remains constant with respect to time, as a consequence, $\tau = -\frac{\ln(\mathcal{U})}{c\Sigma_t^i} = -\frac{\ln(\mathcal{U})}{c\sigma_t^{n,i}}$ is simple to sample.

- For the semi-analog MC scheme, neither the expression of the weight modification nor the expression of the collision time require any additional approximation. For this reason, the **semi-analog MC scheme will be chosen for the next computations** even if known to have a slightly bigger variance than the non-analog MC scheme (see [16] section 9.7).

Note that in an HPC context in which *replication domain*¹⁴ (see [18]) is intensively

¹⁴*Replication domain* consists in replicating the geometry on several processors and tracking several MC particles populations with different initial seeds in every replicated domains. At the end of the time steps, the contribution of every processors are averaged. This parallel strategy is particularly well suited to MC codes, taking advantage of the independence of the MC particles.

applied, this excess of variance is quite easy to compensate: with a small increase of replicated domains, we can easily absorb the excess of variance of the semi-analog MC scheme (intensively used in neutronics for example, and called *implicit capture* see [26]) with respect to the non-analog MC one. Of course, asymptotically with the number of MC particles, both the non-analog and the semi-analog MC schemes for (16) converge toward the solution of (16).

- Of course, the *analog* MC scheme could be used (or even others, some of them probably even more relevant), but this is beyond the scope of this paper. We here focus on MC scheme which can be found in legacy IMC codes.

To end the time step, it remains to detail the track length estimator needed to consistently update the material energy from equation (7b), see point (**), page 5. By consistent tally, we here aim at having a conservative scheme. In order to ensure conservativity for the system 'photons+matter', each time a collision occurs, we make sure that matter tallies, in cell i , from particle p ,

$$\begin{aligned}
\Delta E_p^i &= (w_p(\tau^-) - w_p(\tau^+)) \mathbf{1}_{\Omega_i}(x_p(\tau)), \\
&= w_p(\tau^-) \underbrace{\left(1 - \frac{\Sigma_S^i(\tau)}{\Sigma_t^i(\tau)}\right)}_{\Delta e_p^i} \mathbf{1}_{\Omega_i}(x_p(\tau)), \\
&= w_p(\tau^-) \left(1 - \frac{\frac{S^i}{U^i(\tau)} + c\Sigma_s^i}{c\Sigma_t^i}\right) \mathbf{1}_{\Omega_i}(x_p(\tau)), \\
&= \frac{w_p(\tau^-)}{c\Sigma_t^i} \left(c\Sigma_a^i - \frac{S^i}{U^i(\tau)}\right) \mathbf{1}_{\Omega_i}(x_p(\tau)).
\end{aligned} \tag{20}$$

Note that in above expression, τ^- (respectively τ^+) denotes the time just before (respectively after) the collision occurring at time τ . We insist the notations above are in agreement with the fact that the contribution of particle p is zero if particle p does not encounter a collision within cell i . Of course, the matter energy within each cell i is updated by tallying every (non-zero) contributions of every MC particles within cell i as $E_i^n = E_i^0 + \sum_{p=1}^{N_{MC}} \Delta E_p^i$. The last expression allows ending the description of the scheme.

Remark 4.2. *Note that the MC scheme described here to solve (13) is general enough and could benefit other physics (neutronics for example, see [24]).*

The new MC scheme we just described is called, for the sake of conciseness, nssIMC (for *no source sampling IMC*) in the following paragraphs. We next take some time describing some of its singular properties. We would like to decompose the discussion into two points:

- the first point concerns *continuous* considerations. We compare the stake of having to resort to IMC or nssIMC asymptotically as $N_{MC} \rightarrow \infty$:
 - IMC solves (13) with $\Phi^n(x) = \Phi_{approx}^n + \mathcal{O}(\delta_x)$ leading to the discretisation of (8)–(9),
 - whereas nssIMC solves (13) assuming $\frac{S}{I} = \frac{S}{I} + \mathcal{O}(\epsilon)$ leading to the discretisation of (16).

We will study the extent of this $\mathcal{O}(\epsilon)$ approximation on $\frac{S}{I}$ just as we studied the extent of the $\mathcal{O}(\delta_x)$ approximation on Φ^n for IMC in [2].

- The second point aims at focusing on the MC discretisations. IMC usually uses a non-analog MC scheme to discretise (8)–(9). With nssIMC, as explained above, we can either use the previously presented non-analog MC scheme or the semi-analog one to discretise (16). In this second point, we compare the non-analog IMC scheme and the non-analog¹⁵ nssIMC one. We comment on the operations and restrictions induced by both schemes.

Let us begin by the first point above and the comparison of the continuous equations (13) and (16): (16) has been built from (13) with the linearisation hypothesis of remark 4.1, consisting in plugging the solution of equation (14) within (13). This choice has been driven by the fact that

- the source term is treated within the solution of (13) (without source sampling),
- and by the fact that an accurate and cheap solution, given by (15), is available for (14).

We here want to insist on the fact that the choice of resorting to the homogeneous equation (14) as a reduced model, motivated mainly by the above two *practical* considerations, may not be the best choice to capture of the equilibrium diffusion limit¹⁶. To better understand what happens, let us first rewrite (13) in term of nondimensional quantities (uperscript * will be used to denote them). Introduce

$$\begin{cases} x = x^* \mathcal{X}, c = c^* \mathcal{C}, t = t^* \mathcal{T}, \\ \Sigma_\alpha = \Sigma_\alpha^* \frac{1}{\Lambda_\alpha}, \forall \alpha \in \{s, t, a\}, \end{cases} \quad (21)$$

together with $I^*(x^*, t^*, \omega) = I(x, t, \omega)$ and $S^*(x^*, t^*) = S(x, t) = c \Sigma_a \Phi^n(x)$. Then by noticing that

$$\frac{1}{\mathcal{T}} \partial_{t^*} I^*(x^*, t^*, \omega) = \partial_t I(x, t, \omega), \quad \frac{1}{\mathcal{X}} \partial_{x^*} I^*(x^*, t^*, \omega) = \partial_x I(x, t, \omega),$$

(13) can be equivalently rewritten (we drop the dependences for conciseness)

$$\partial_{t^*} I^* + \frac{\mathcal{CT}}{\mathcal{X}} c^* \omega \cdot \nabla_{x^*} I^* + \left[\frac{\mathcal{CT}}{\Lambda_s} c^* \Sigma_s^* + \frac{\mathcal{CT}}{\Lambda_a} c^* \Sigma_a^* \right] I^* = \frac{\mathcal{TC}}{\Lambda_a} c^* \Sigma_a^* \Phi^{n,*} + \frac{\mathcal{CT}}{\Lambda_s} c^* \Sigma_s^* \int_{4\pi} I^* \frac{d\omega'}{4\pi}.$$

The homogeneous equation (14) can be recovered from the above expression assuming

$$\begin{aligned} \frac{\mathcal{CT}}{\mathcal{X}} &= \mathcal{O}(\epsilon) = \frac{\mathcal{CT}}{\Lambda_s}, \\ \frac{\mathcal{CT}}{\Lambda_a} &= \mathcal{O}(1), \end{aligned} \quad (22)$$

with $\epsilon \sim 0$ small. With the above nondimensional quantities, we can have an idea of what (16) misses with respect to (13) (first bullet below) and compare regimes characterised by ϵ with (22) and δ with (3) (second bullet below).

¹⁵In the next numerical section 5, we do use the semi-analog MC scheme for (16) for the practical reason previously exposed. But it is way easier comparing both non-analog MC schemes on the paper. This does have a sense as both semi-analog and non-analog MC scheme recover asymptotically the same solution: the comments on the non-analog nssIMC can be transposed, without loss of generality, to the semi-analog nssIMC one.

¹⁶Still, it does cancel the teleportation error.

- Let us first compare more quantitatively (13) and (16): this can be done performing a Hilbert development [27] of $I^* = I_0 + \epsilon I_1 + \epsilon^2 I_2 + \mathcal{O}(\epsilon^3)$, plugging it in (13) and identifying the equations satisfied by the leading order I_0 :

$$\begin{cases} \mathcal{O}(1) & \partial_t I_0 + c\Sigma_a I_0 - S = 0, \\ \mathcal{O}(\epsilon) & \dots \end{cases}$$

From the first equation, we recover that I_0 coincides with U (given the same initial conditions). This means that

$$\begin{aligned} I_0 = U &= \frac{S}{c\Sigma_a} + e^{-c\Sigma_a t} \left(U_0 - \frac{S}{c\Sigma_a} \right), \\ &= \Phi^n + e^{-c\sigma_a^n f^n t} (U_0 - \Phi^n), \end{aligned} \quad (23)$$

where x, ω are only parameters. Of course we could go further in the development but the first order is enough for the rest of the discussion. We can then replace I by $U + \epsilon I_1 + \mathcal{O}(\epsilon^2)$ in (13) to get

$$\begin{aligned} \partial_t I + c\omega \cdot \nabla I + c\Sigma_t I &= \int_{4\pi} \left(\frac{S}{I} + c\Sigma_s \right) I \frac{d\omega'}{4\pi}, \\ &= \int_{4\pi} \left(\frac{S}{I_0 + \epsilon I_1 + \mathcal{O}(\epsilon^2)} + c\Sigma_s \right) I \frac{d\omega'}{4\pi}. \end{aligned} \quad (24)$$

Performing the development as $\epsilon \sim 0$ finally leads to

$$\underbrace{\partial_t I + c\omega \cdot \nabla I + c\Sigma_t I}_{(16)} = \underbrace{\int_{4\pi} \left(\frac{S}{U} + c\Sigma_s \right) I \frac{d\omega'}{4\pi}}_{(13)} - \underbrace{\epsilon \int_{4\pi} \left[S \frac{I_1}{U^2} \right] I \frac{d\omega'}{4\pi}}_{K_1} + \mathcal{O}(\epsilon^2). \quad (25)$$

what (16) misses w.r.t. (13)

With the above equation, we characterised what is missed when solving (16) instead of (13). Let us briefly study K_1 :

$$\begin{aligned} K_1(x, t) &= \int_{4\pi} c\sigma_a^n(x) f^n(x) \Phi^n(x) \frac{I_1(x, t, \omega')}{U^2(x, t)} I(x, t, \omega') \frac{d\omega'}{4\pi}. \\ &= \int_{4\pi} c\Sigma_\epsilon(x, t, \omega') I(x, t, \omega') \frac{d\omega'}{4\pi}. \end{aligned} \quad (26)$$

At first order with $\mathcal{O}(\epsilon)$, (16) lacks a kind of scattering term. We will need its expression in the next point below.

- Let us finally study how hypothesis (22) impacts the equilibrium diffusion limit. For this, just as in [2] in which we performed both a Hilbert development with respect to δ and a Taylor one with respect to δ_x in the IMC linearisation (7), we suggest performing a Hilbert development with respect to δ and a Taylor one with respect to ϵ in (7). The calculation are somewhat easier than in [2] because ϵ does not affect the Fleck factor as δ_x does (see [2]).

With nssIMC, on time step $[0, t = \Delta t]$, we aim at solving the conservative system

$$\begin{cases} \partial_t I + c\omega \cdot \nabla I + c\sigma_t^n I = \int_{4\pi} \left[cf^n \sigma_a^n \frac{\Phi^n}{U} + c(\sigma_s^n + (1 - f^n)\sigma_a^n) \right] I \frac{d\omega'}{4\pi}, \end{cases} \quad (27a)$$

$$\begin{cases} \partial_t E = cf^n \sigma_a^n \int_{4\pi} \frac{I}{4\pi} \left(1 - \frac{\Phi^n}{U} \right) d\omega. \end{cases} \quad (27b)$$

Let us first make the Taylor development with respect to ϵ appear in (27): the previous calculations showed that $U = I - \epsilon I_1 + \mathcal{O}(\epsilon^2)$. Plugging $U = I - \epsilon I_1 + \mathcal{O}(\epsilon^2)$ into (27) leads to

$$\begin{cases} \partial_t I + c\omega \cdot \nabla I + c\sigma_t^n I = cf^n \sigma_a^n \Phi^n + c[\sigma_s^n + (1 - f^n)\sigma_a^n] \int_{4\pi} I \frac{d\omega'}{4\pi} + K_1 \epsilon + \mathcal{O}(\epsilon^2), \end{cases} \quad (28a)$$

$$\begin{cases} \partial_t E = cf^n \sigma_a^n \left(\int_{4\pi} \frac{I}{4\pi} d\omega - \Phi^n \right) - K_1 \epsilon + \mathcal{O}(\epsilon^2). \end{cases} \quad (28b)$$

Let us now perform a Hilbert development¹⁷ of $I = I^0 + \delta I^1 + \mathcal{O}(\delta^2)$ with respect to δ into, first, K_1 . Few calculations using the expression (23) in (26) lead to:

$$\begin{aligned} \epsilon K_1 &\underset{\delta \sim 0}{\sim} \epsilon \delta^2 \quad I_1^0 \frac{\Phi^n}{\beta^n \Delta t (\Phi^n + e^{-\frac{t}{\beta^n \Delta t}} (-\Phi^n + U_0))} + \mathcal{O}(\delta^4) + \mathcal{O}(\epsilon^2), \\ &\underset{\delta \sim 0}{\sim} \epsilon \delta^2 \quad K_1^0 + \mathcal{O}(\delta^4) + \mathcal{O}(\epsilon^2), \end{aligned}$$

If we now perform the Hilbert development of I with respect to δ satisfying (3) and identify the leading orders in the first equation of (28), we obtain¹⁸

$$\begin{aligned} \mathcal{O}(\delta^0) : \quad & I^0 = \int_{4\pi} I^0 \frac{d\omega}{4\pi} = \Phi_r^0, \\ \mathcal{O}(\delta^1) : \quad & c\omega \cdot \nabla I^0 + c\sigma_t I^1 = 0, \\ \mathcal{O}(\delta^2) : \quad & \partial_t I^0 + \int_{4\pi} c\omega \cdot \nabla I^1 \frac{d\omega}{4\pi} = \frac{1}{\Delta t \beta^n} (I^0 - \Phi^{n,0}) + \epsilon K_1^0 + \mathcal{O}(\epsilon^2). \end{aligned}$$

Performing the same calculations on the second equation of (28) leads to

$$\mathcal{O}(\delta^2) : \quad \partial_t E^0 = -\frac{1}{\Delta t \beta^n} (I^0 - \Phi^{n,0}) - \epsilon K_1^0 + \mathcal{O}(\epsilon^2).$$

Finally for nssIMC, during an arbitrary time step $[t^n, t^{n+1}]$, as $N_{MC} \rightarrow \infty$, at leading order with respect to δ **and** ϵ in the equilibrium diffusion regime characterised by (3), system (7) behaves like¹⁹

$$\begin{cases} \partial_t (E + \Phi_r) - \nabla \left(\frac{c}{3\sigma_t^n} \nabla \Phi_r \right) = \mathcal{O}(\epsilon^2) + \mathcal{O}(\delta), \\ \partial_t E = \frac{1}{\beta^n \Delta t} [\Phi_r - \Phi^n] - \frac{\epsilon I_1^0 \Phi^n}{\beta^n \Delta t (\Phi^n + e^{-\frac{t}{\beta^n \Delta t}} (-\Phi^n + U_0))} + \mathcal{O}(\delta) + \mathcal{O}(\epsilon^2). \end{cases} \quad (29)$$

¹⁷Note that the upperscripts are relative to the δ development whereas the lowerscripts are relative to the ϵ one.

¹⁸The calculations are similar to the ones performed in [6, 2]. The last equation is integrated with respect to ω .

¹⁹We drop the ⁰ upperscripts for convenience.

The limit equation (29) for nssIMC must be compared to (10) for IMC and to (11) for ISMC. Note that with $\epsilon = 0$, the analysis recovers the one of [6] for IMC (without spatial discrepancy δ_x). The nssIMC linearisation ensures cancelling δ_x induced by source sampling within the IMC linearisation. For this reason, we consider nssIMC is a teleportation error free²⁰ MC solver for (7). But nssIMC has to deal with a different type of error $\mathcal{O}(\epsilon)$. At first glance, (29) does not necessarily look better than (10) with $k = 1$ or $k = 2$ (i.e. IMC and tilted IMC). The first equation of (29) is a diffusion equation with the good $\frac{c}{3\sigma_t}$ coefficient. But the equilibrium equation is perturbed by the $\mathcal{O}(\epsilon)$ term. As Δt goes to zero, the second equation of (29) behaves as

$$\mathcal{O}(\Delta t) = \Phi_r - \Phi^n - \epsilon I_1^0.$$

Of course, if ϵ or I_1^0 are small, then equilibrium is recovered. Otherwise, it is not fulfilled. It is certainly still possible to consider higher order reduced models with respect to ϵ , i.e. try to build²¹ a *tilt* $I = U + \mathcal{O}(\epsilon^k)$ with $k > 1$ with respect to ϵ . Or we could rely on a reduced model based on better suited hypothesis than (22). These possible extensions are beyond the scope of this paper but attest that nssIMC could be improved thanks to quite classical methods.

At this stage of the discussion, one natural question remains: is having an $\mathcal{O}(\epsilon)$ error really better than having an $\mathcal{O}(\delta_x)$ one? The benchmarks of section 5 tend to show that the $\mathcal{O}(\epsilon)$ term is preferable on coarse meshes.

Let us tackle the second point and the implications of having to resort to the non-analog nssIMC scheme for (16) instead of the non-analog IMC one for (8)–(9). These are more practical considerations about not relying on source sampling anymore. With this new MC solver, there is not anymore a distinction between ‘initial’ and ‘source’ particles as with IMC. The weight of each MC particle with nssIMC takes the source term into account. Let us focus on the weight modification and the particle to matter contribution. For this, we suggest comparing their expressions for an IMC particle and for an nssIMC particle:

- for the (non-analog) IMC solver, the weight modification is

$$w_p(t) = w_p(0)e^{-c\Sigma_a^i t} \geq 0.$$

It is a decreasing quantity (as $\Sigma_a^i \geq 0$). The contribution to matter of the same particle p is given by

$$\Delta E_p^i(t) = w_p(0)(1 - e^{-c\Sigma_a^i t}) = w_p(0)\Delta e_p^i(t) \geq 0.$$

As $\Sigma_a^i \geq 0$, the weight of an IMC particle can only decrease and lead to a conservative increase of the matter energy. At the end of a time step $[0, t = \Delta t]$, the update of the matter energy is given by²²

$$E_i(t) = E_i^0 - c\sigma_a^0 f^0 \beta^0 \Delta t + \sum_{p=1}^{N_{MC}} \sum_{j=1}^{N_p} w_p(t_p^j) \Delta e_p^i(t_p^{j+1} - t_p^j), \quad (30)$$

²⁰ISMC is an implicitation of SMC, see [8, 2], which by construction is a teleportation error free solver.

²¹Just as tilted IMC consider higher orders of $\Phi^n(x) = \Phi_{approx}^n(x) + \mathcal{O}(\delta_x^{k>1})$ with respect to δ_x .

²²One can check that in a closed cell, every time intervals become (only interval) $[0, t]$ and conservativity is ensured.

where $[t_p^j, t_p^{j+1}]_{i \in \{1, \dots, N_p\}}$ denotes N_p intervals of time spent by particle p within cell i . The positiveness of the energy $E_i(t)$ at the end of the time step is ensured provided a small enough time step which can be prescribed *a priori*: it is enough choosing $\Delta t \leq \frac{E_i^0}{c\sigma_a^0 f^0 \beta^0}$, (remember each $\Delta e_p^i(t) \geq 0$). It may be too constraining/suboptimal: for example, in a configuration with important incoming particle to matter contributions in cell i , bigger time step could be used and still ensure positiveness.

- For the nssIMC solver, it is easy checking that if $U_0^i, \Sigma_a^i, \Sigma_s^i, c, S^i$ are all positive quantities, the weight (18)

$$w_p(t) = w_p(0) \left(e^{-c\Sigma_a^i t} + S^i \frac{1 - e^{-c\Sigma_a^i t}}{c\Sigma_a^i U_0^i} \right) \geq 0,$$

remains positive. But *it is not necessarily decreasing* as for IMC. Indeed, if emission compensates absorption, which occurs as soon as $S^i - c\Sigma_a^i U_0^i > 0$ independently of the time step, emission is preponderant and the weight of a particle traveling within cell i increases. The contribution to matter of the same particle p is given by

$$\Delta E_p^i(t) = w_p(0) \left(1 - \left(e^{-c\Sigma_a^i t} + S^i \frac{1 - e^{-c\Sigma_a^i t}}{c\Sigma_a^i U_0^i} \right) \right) = w_p(0) \Delta e_p^i(t), \quad (31)$$

and is conservative but unsigned. In fact, $\Delta e_p^i(t)$ is

- positive $0 \leq \Delta e_p^i(t) < 1 - \frac{S^i}{c\Sigma_a^i U_0^i}$ if absorption is preponderant (if $S^i - c\Sigma_a^i U_0^i \leq 0$),
- negative $0 > \Delta e_p^i(t) > 1 - \frac{S^i}{c\Sigma_a^i U_0^i}$ if emission is preponderant (if $S^i - c\Sigma_a^i U_0^i > 0$),

independently of the time step.

The matter energy at the end of the time step $[0, t = \Delta t]$ is given by

$$E_i(t) = E_i^0 + \sum_{p=1}^{N_{MC}} \sum_{j=1}^{N_p} w_p(t_p^j) \Delta e_p^i(t_p^{j+1} - t_p^j),$$

where $[t_p^j, t_p^{j+1}]_{i \in \{1, \dots, N_p\}}$ denotes N_p intervals of time spent by particle p within cell i . One can check that in a closed cell, every time intervals become (only interval) $[0, t]$ and conservativity is ensured.

From the above expression, we can see that in an emissive cell i ($S^i - c\Sigma_a^i U_0^i > 0$), the sum of negative particle contributions can make $E_i(t)$ become negative. The positive and negative contributions are not as decoupled as in the IMC formalism, see (30). As a consequence, from (31), it is possible in practice

- (a) to have an estimation of the time step limitation $\Delta t \leq \Delta t_{\max}$ needed in order to make sure that $\forall j \in \{1, \dots, N_p\}$, $\Delta e_p^i(t_p^{j+1} - t_p^j)$ remain greater (because negative) than a prescribed quantity Δe_p^{\min} :

$$\Delta t \leq \Delta t_{\max} = -\frac{1}{c\Sigma_a^i} \ln \left(\frac{S^i + (\Delta e_p^{\min} - 1)U_0^i c\Sigma_a^i}{S^i - U_0^i c\Sigma_a^i} \right).$$

Just as for IMC, this limitation may be suboptimal.

- (b) nssIMC also allows another possibility: for a fixed time step $t = \Delta t$, it is possible to limit the maximum initial weight $\max_p(w_p(0)) = \frac{\Delta E_p^{\min}}{\Delta e_p^i(t)}$ of each particle p so that $\Delta E_p^i(t)$ remains below a prescribed value $w_p(0)\Delta e_p^i(t) \leq \Delta E_p^{\min}$.

The previous points (a) time step limitation and (b) weight limitation constitute our main levers to ensure the positiveness of the matter energy at the end of the time step for nssIMC.

We now suggest implementing nssIMC and comparing it to IMC and ISMC on some benchmarks from the literature. To give an idea of the minimal modifications needed to implement the new MC scheme within a legacy IMC code, we rely on algorithm 1 in Appendix C.

5. Numerical results

In this section, we first compare our new IMC solver with the ISMC solver [2] on the Marshak wave test-case presented in [7]. It is, to our knowledge, the only benchmark of the literature putting forward the competing behaviour between the spatial and time discretisation (i.e. with a convergence study with respect to Δt for a fixed spatial discretisation). The new solver is called nssIMC (for *no source sampling IMC*) for conciseness. The results obtained with nssIMC are displayed figure 3. They can be directly compared to the results of figure 1 for IMC (without tilt)

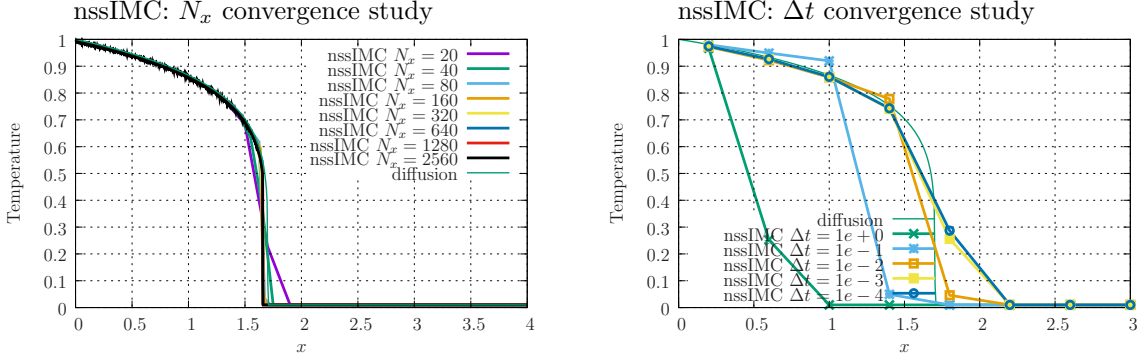


Figure 3: Convergence studies on the material temperature profiles $T(x, t^* = 500)$ at $t^* = 500$ for the nssIMC scheme, with respect to $N_x = \{20, 40, 80, 160, 320, 640, 1280, 2560\}$ and $\Delta t = 5 \times 10^{-3}$ (left) and to $\Delta t \in \{10^0, 10^{-1}, 10^{-2}, 10^{-3}\}$ and $N_x = 10$ (right).

and of figure 2 for ISMC.

First, comparing figures 3 (left) and 1 (left) allows highlighting the gain of the nssIMC scheme with respect to IMC: the spatial convergence is fast once source sampling is avoided (i.e. once we make sure $\delta_x = 0$ by construction): indeed, every spatial discretisation (from the coarser $N_x = 20$ to the finer $N_x = 2560$) allows recovering the reference solution. The ISMC scheme, see figure 2 (left), already exhibited such fast spatial convergence (it is also, by construction, such that $\delta_x = 0$, see [2]). In this sense, the nssIMC scheme allows cancelling the teleportation error.

On another hand, the right pictures of figures 1–2–3 display a convergence study with respect Δt for fixed spatial discretisation $N_x = 10$ (coarse mesh, as in [7] from which the benchmark is taken) and for fixed number of MC particles (up to source sampling fluctuations for the IMC solver). First,

the IMC solver exhibits a *diverging* behaviour with respect to Δt (intensively studied in [2]), see figure 1 (right). This diverging behaviour is explained by the appearance of a numerical advection term (see (10) for $k = 1$ and [2] and remark 3.1). On another hand, the new nssIMC does not exhibit this diverging behaviour with respect to Δt . On the contrary, the behaviour is converging: the finer the time step, the closer to the reference solution the nssIMC solution is, see figure 3 (right). But the convergence with respect to Δt is slower than for the ISMC scheme for which every curves with every time steps are undistinguishable from one another, see figure 2. This is another point in favor of ISMC: it seems to have a faster Δt -convergence rate than nssIMC. Still, both teleportation error free solvers, ISMC and nssIMC, do not present the competing behaviour between the spatial and the time discretisation defined in remark 3.1.

The next benchmark is taken from [2]. Its description is given in Appendix B. From now on, we only *display* the results obtained from ISMC and the new nssIMC solvers (and rely on [2] for IMC vs. ISMC comparisons).

Let us begin by some Δt convergence studies and ISMC vs. nssIMC comparisons. These are displayed figure 4: the left column presents ISMC results and the right column presents the nssIMC ones for $N_x = 40$ cells²³, $N_{MC} = 8.8 \times 10^5$ and several time steps $\Delta t = \{5 \times 10^{-9}, 10^{-10}, 10^{-11}, 10^{-12}\}$. For the coarser time step $\Delta t = 5 \times 10^{-9}$, as expected from (11) for ISMC and (29) for nssIMC, equilibrium is not fulfilled. For a finer time step $\Delta t = 10^{-10}$, ISMC already ensures capturing the equilibrium diffusion limit. On another hand, the time step is too coarse for nssIMC to give as good results as ISMC. But for the last time steps, $\Delta t = 10^{-11}$ and $\Delta t = 10^{-12}$, both ISMC and nssIMC presents accurate results with respect to the reference solution, even if nssIMC seems to be slightly noisier. For $\Delta t = 10^{-10}$ and nssIMC, the plot display a mix between numerical noise from the MC discretisation and numerical instabilities due to a too coarse time step. Once Δt below 10^{-11} , only remains numerical noise from the MC discretisation. The fact that the $\Delta t = 10^{-12}$ curve seems to be noisier than the $\Delta t = 10^{-11}$ is only due to (a lack of?) luck. For different initial random seeds, the curves could have been smoother or even seem less noisy for $\Delta t = 10^{-12}$ than for $\Delta t = 10^{-11}$.

Figure 5 presents a spatial convergence study for both ISMC and nssIMC for fixed time step $\Delta t = 10^{-12}$. On the first line of figure 5, the curves for $N_x = 20$ and $N_{MC} = 8.8 \times 10^5$ are displayed. Both curves testify to a fast spatial convergence rate for both ISMC and nssIMC. Still, the results for ISMC are slightly better than for nssIMC: this is visible especially in the vicinity of $x = 0.5$, where nssIMC fail to resolve the peak of temperature as sharply as ISMC. Note that the nssIMC results remain way more accurate than (tilted or not) IMC ones, for both the peak of temperature and the wavefronts, see [2]. Let us consider some more quantitative results:

$N_x = 20$ Let us first consider the peak of temperature (at $x = 0.5$) as an observable of interest. For $N_x = 20$ and $\Delta t = 10^{-12}$, the different solvers give²⁴²⁵

²³Note that there are $N_x = 40$ cells instead of only 20 as in [2].

²⁴Note that the results from IMC are not displayed but can be found in [2].

²⁵Note that the results tilted IMC are not displayed but can be found in [2].

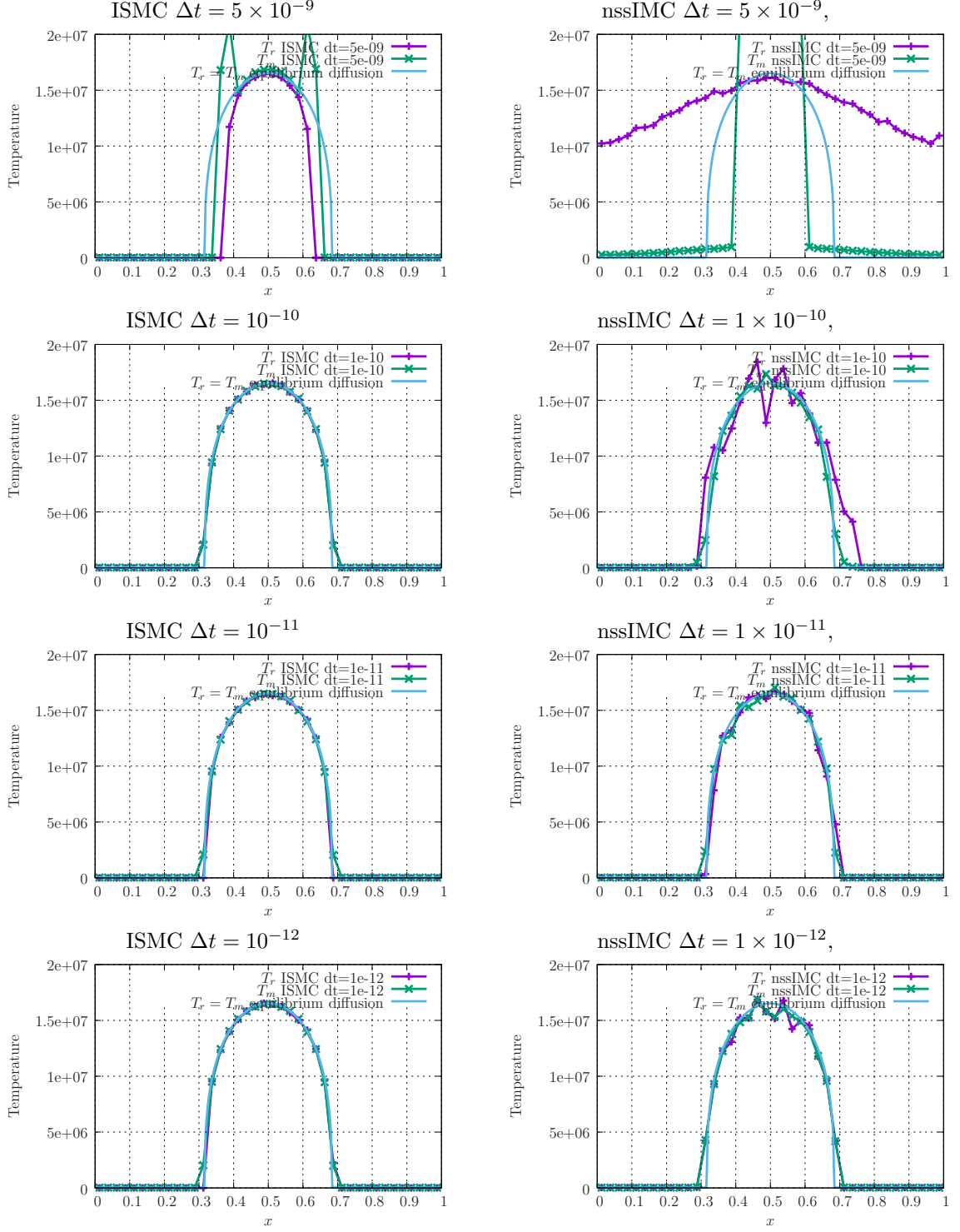


Figure 4: Comparisons of the material and radiative temperatures T_m and T_r obtained from (reference solution) a deterministic solver for the equilibrium diffusion limit (2), the ISMC and the nssIMC approximations for $N_x = 40$, $N_{MC} \approx 8.8 \times 10^5$ MC particles and $\Delta t = \{5 \times 10^{-9}, 10^{-10}, 10^{-11}, 10^{-12}\}$.

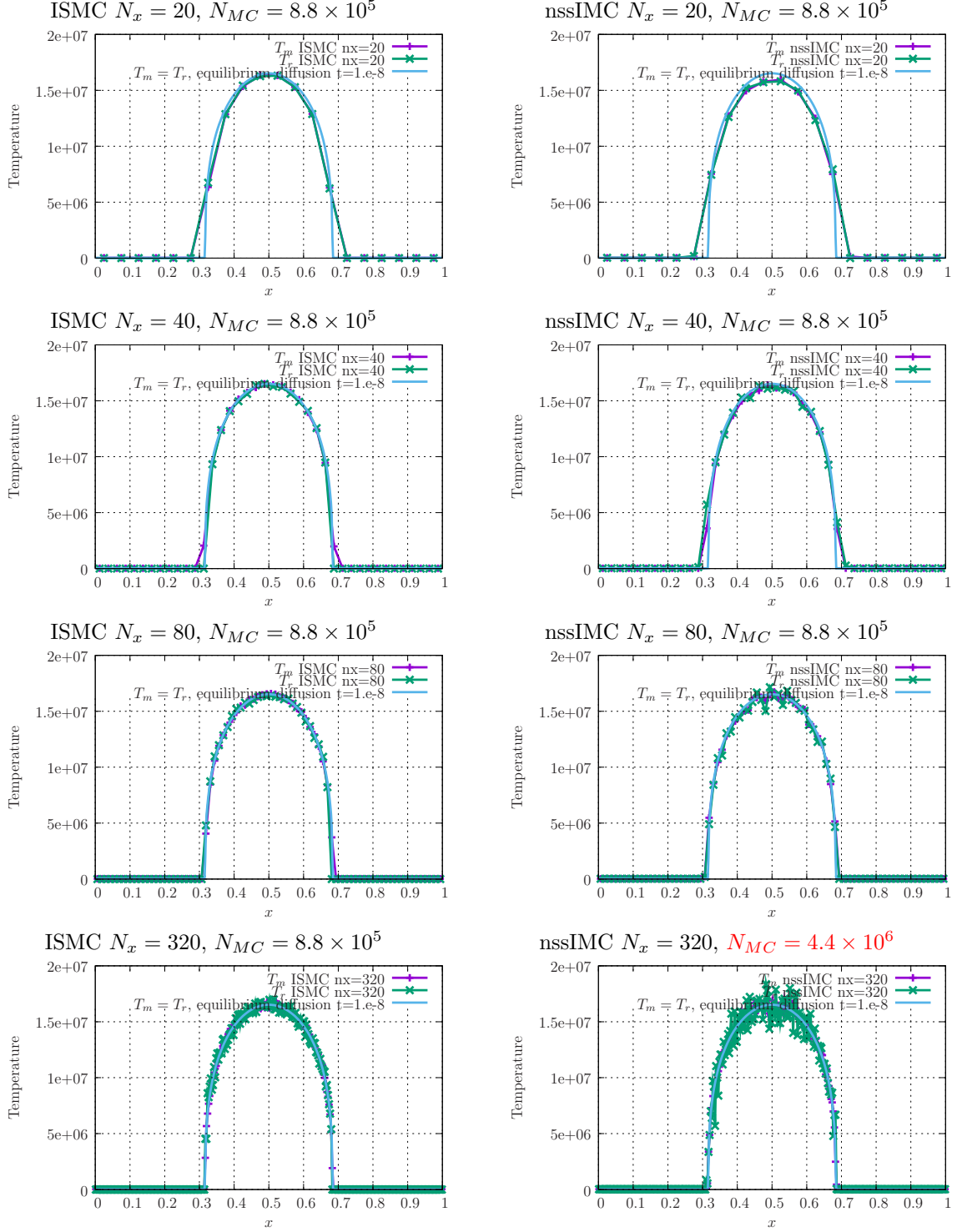


Figure 5: Comparisons of the material and radiative temperatures T_m and T_r obtained from (reference solution) a deterministic solver for the equilibrium diffusion limit (2), the ISMC and the nssIMC approximations for $N_x \in \{20, 40, 80, 160, 320\}$, $\Delta t = 10^{-12}$ and $N_{MC} \approx 8.8 \times 10^5$ MC particles (except for nssIMC $N_x = 320$ for which we needed $N_{MC} = 4.4 \times 10^6$).

- diffusion: $T(t = 10^{-8}, x = 0.5) = 1.652136 \times 10^7$ (reference),
- IMC: $T(t = 10^{-8}, x = 0.5) = 7.642123 \times 10^6$ with a relative error of 53.74,
- tilted IMC: $T(t = 10^{-8}, x = 0.5) = 1.187466 \times 10^7$ with a relative error of 28.12,
- ISMC: $T(t = 10^{-8}, x = 0.5) = 1.630483 \times 10^7$ with a relative error of 1.310,
- nssIMC: $T(t = 10^{-8}, x = 0.5) = 1.580614 \times 10^7$ with a relative error of 4.329.

From the above relative error, we can estimate gains on the peak of temperature observables:

- tilted IMC leads to a gain $\times 1.91$ w.r.t. IMC,
- ISMC leads to a gain $\times 41.0$ w.r.t. IMC, $\times 21.4$ w.r.t. tilted IMC,
- nssIMC leads to a gain $\times 12.4$ w.r.t. IMC, $\times 6.49$ w.r.t. tilted IMC.

- Let us now consider the left wavefront x_w ²⁶ as observable. For $N_x = 20$ and $\Delta t = 10^{-12}$, the different solvers give

- diffusion: $x_w(t = 10^{-8}) = 3.130 \times 10^{-1}$ (reference),
- IMC: $x_w(t = 10^{-8}) = 7.500 \times 10^{-2}$, leading to a relative error of 0.76,
- tilted IMC: $x_w(t = 10^{-8}) = 1.125 \times 10^{-1}$, leading to a relative error of 0.64,
- ISMC: $x_w(t = 10^{-8}) = 2.750 \times 10^{-1}$, leading to a relative error of 0.12,
- nssIMC: $x_w(t = 10^{-8}) = 2.750 \times 10^{-1}$, leading to a relative error of 0.12.

From the above relative error, we can estimate gains on the wavefront:

- tilted IMC leads to a gain $\times 1.18$ w.r.t. IMC,
- ISMC leads to a gain $\times 6.26$ w.r.t. IMC, $\times 5.27$ w.r.t. tilted IMC,
- nssIMC leads to a gain $\times 6.26$ w.r.t. IMC, $\times 5.27$ w.r.t. tilted IMC.

$N_x = 40$

Let us once again consider the peak of temperature (at $x = 0.5$) as an observable of interest.

For $N_x = 40$ and $\Delta t = 10^{-12}$, the different solvers give^{27,28}

- diffusion $T(t = 10^{-8}, x = 0.5) = 1.652136 \times 10^7$ (reference),
- IMC $T(t = 10^{-8}, x = 0.5) = 8.792122 \times 10^6$ with a relative error of 0.467,
- tilted IMC $T(t = 10^{-8}, x = 0.5) = 1.579830 \times 10^7$ with a relative error of 0.044,
- ISMC $T(t = 10^{-8}, x = 0.5) = 1.622959 \times 10^7$ with a relative error of 0.017,
- nssIMC $T(t = 10^{-8}, x = 0.5) = 1.613410 \times 10^7$ with a relative error of 0.023.

From the above relative error, we can estimate gains on the peak of temperature observables:

- tilted IMC leads to a gain $\times 10.68$ w.r.t. IMC,
- ISMC leads to a gain $\times 26.49$ w.r.t. IMC, $\times 2.47$ w.r.t. tilted IMC,
- nssIMC leads to a gain $\times 19.95$ w.r.t. IMC, $\times 1.86$ w.r.t. tilted IMC.

- Let us now consider the left wavefront x_w ²⁹ as observable. For $N_x = 40$ and $\Delta t = 10^{-12}$, the different solvers give

- diffusion $x_w(t = 10^{-8}) = 3.130 \times 10^{-1}$ (reference),
- IMC $x_w(t = 10^{-8}) = 1.625 \times 10^{-1}$, leading to a relative error of 0.481,
- tilted IMC $x_w(t = 10^{-8}) = 2.625 \times 10^{-1}$, leading to a relative error of 0.161,
- ISMC $x_w(t = 10^{-8}) = 3.125 \times 10^{-1}$, leading to a relative error of 0.001,
- nssIMC $x_w(t = 10^{-8}) = 2.875 \times 10^{-1}$, leading to a relative error of 0.081.

From the above relative error, we can estimate gains on the wavefront:

²⁶i.e. the last cell in which the radiative temperature T_r is different than the initial temperature.

²⁷Note that the results from IMC are not displayed but can be found in [2].

²⁸Note that the results from tilted IMC are not displayed but can be found in [2].

²⁹i.e. the last cell in which the radiative temperature T_r is different than the initial temperature.

- tilted IMC leads to a gain $\times 2.983$ w.r.t. IMC,
- ISMC leads to a gain $\times 301.0$ w.r.t. IMC, $\times 101.0$ w.r.t. tilted IMC,
- nssIMC leads to a gain $\times 5.901$ w.r.t. IMC, $\times 1.980$ w.r.t. tilted IMC.

The previous quantitative results are displayed for $N_x = 20$ and $N_x = 40$ mainly because finer meshes would need much more MC particles to avoid having noisy results. Besides, we are more interested in the gains on coarse meshes (the ones which are practically of interest for production codes). Let us comment on the previous gains on the temperature peak and on the wavefront: first, *nssIMC always ensures gains with respect to both IMC and tilted IMC, on both observables and both grids*: from $\times 5.901$ up to $\times 19.95$ with respect to IMC and from $\times 1.86$ up to $\times 6.49$ for tilted IMC. As already qualitatively put forward on figure 5, ISMC does generate even better gains: from $\times 6.26$ up to $\times 301.0$ with respect to IMC and from $\times 2.47$ up to $\times 101.0$ with respect to tilted IMC. On figure 5, for $N_x = 40$ and $N_x = 80$, both teleportation error free solvers present accurate results, even if nssIMC seems to be slightly noisier. The curves and quantitative results tend to show ISMC spatially converges faster than nssIMC. Note that this point³⁰ could be investigated more thoroughly but we think the spatial convergence of nssIMC deserves more attention, mainly because of the results of the last line of figure 5: on the last line of figure 5 are displayed the results obtained with ISMC and nssIMC with $N_x = 320$ but with different number of MC particles N_{MC} (N_{MC} is recalled in red for nssIMC). The computation for nssIMC with $N_{MC} = 8.8 \times 10^5$ failed to run: negative matter energies were produced by the nssIMC. The problem anticipated in section 4 occurs in practice. Recall that ISMC, on another hand, is a positive scheme³¹. Now, with nssIMC, using more MC particles ($N_{MC} = 4.4 \times 10^6$, see point (b) at the end of section 4) leads to more robust calculations, as predicted by the discussion.

In practice, the previously described robustness problem could probably be lessened by astute strategies: the element of solution presented at the end of section 4 are relevant. We already used the weight limitation (point (b)). Using splitting *on-the-fly* at the collision to prevent the weight from increasing too much could be even more efficient. But the comparisons between ISMC and nssIMC would not be fair anymore (different numbers of MC particles). Clever time step limitations (point (a)) are also efficient. But once again, the comparisons with ISMC et IMC would not anymore be in the same conditions. We could consider plugging the solution U of a more relevant reduced model than (14), fitted to regime (3), within (13). In practice, such reduced model may not have an analytical solution: its use within a legacy IMC implementation would remain possible (see [24] in which an ODE solver is embedded within the MC framework) but would probably be much more complex and costly. In other words, the new nssIMC solver can certainly be improved thanks to more or less classical strategies (splitting, time step limitation, more relevant reduced model, tilts with respect to ϵ , see the discussion at the end of section 4). But our objective here is to compare the nssIMC and the ISMC linearisations/solvers on common grounds and ISMC presents the advantage of avoiding those additional considerations. Improving nssIMC is therefore beyond the scope of this paper.

³⁰The faster spatial convergence rate of ISMC with respect to nssIMC.

³¹As soon as the modified Fleck factor is positive, the artificial opacities are positive and the MC scheme to discretise both photons and matter ensure the positiveness of both quantities for stable calculations, see [2].

6. Conclusion

In this paper, we presented a new and original Monte-Carlo scheme to cancel the teleportation error and its drawbacks (competing behaviours between the time and spatial discretisation parameters as defined and illustrated in section 3, remark 3.1) within an IMC framework for photonics. Care has been taken to highlight how minimal modifications to an already existing legacy IMC implementation can be made to recover the results of this paper.

The main idea is to avoid having to resort to source sampling to solve the transport equation resulting from the IMC linearisation of the model. For this, a reduced model which can be analytically solved and takes into account the source term is introduced and plugged in to the IMC transport equation. The source term is consequently taken into account *on-the-fly* during the MC resolution. The resulting scheme is conservative, converging but demands an additional linearisation hypothesis (if compared to IMC with source sampling or ISMC for example).

The modified IMC solver, as expected, cancels the teleportation error. The corrections/modifications considerably improve the spatial convergence rate with respect to IMC with source sampling. Benchmarks testify that the time and spatial discretisation parameters are not competing anymore (see remark 3.1).

The new nssIMC (for *no source sampling IMC*) solver is finally numerically compared to the ISMC solver of [2] which also cancels the teleportation error, avoids competing discretisation parameters³² but can not be put into an IMC framework and consequently needs more significant (even if relatively simple) modifications of a code. On the benchmarks of this paper, nssIMC shows a slower convergence rate than ISMC with respect to both the spatial and time discretisations. It even presents some robustness problems which are not encountered with the ISMC scheme (which is positive, under relatively mild conditions on the time step, see [2]). Still, due to the fact that the solver can be implemented with minimal modifications of an IMC implementation and display important gains with respect to IMC, the strategy deserved, in our opinion, to be investigated and documented. Besides, the original (to our knowledge) strategy to take into account a source term *on-the-fly* during the MC resolution (without relying on source sampling) could certainly benefit other solvers/physics.

References

- [1] A. B. Wollaber, Four decades of implicit monte carlo, Journal of Computational and Theoretical Transport (2016).
- [2] G. Poëtte, X. Valentin, A new Implicit Monte-Carlo scheme for photonics (without teleportation error and without tilts), accepted in J. Comput. Phys. (Sep. 2019).
URL <https://hal.archives-ouvertes.fr/hal-02276576>
- [3] J. A. F. Jr., The calculation of nonlinear radiation transport by a monte carlo method, Tech. rep., Lawrence Radiation Laboratory, University of California (1961).
- [4] J. A. Fleck, J. D. Cummings, An implicit monte-carlo scheme for calculating time and frequency dependent nonlinear radiation transport, Journal of Computational Physics (1971).

³²in the sense nssIMC converges as the time step goes to zero for a fixed grid whereas IMC presents a diverging behavior in the same conditions, see the definition in remark 3.1 and the illustration in section 3.

- [5] L. L. Carter, C. A. Forest, Nonlinear radiation transport simulation with an implicit monte carlo method, Tech. rep., Los Alamos National Laboratory (1973).
- [6] J. D. Densmore, E. W. Larsen, Asymptotic equilibrium diffusion analysis of time-dependent monte carlo methods for grey radiative transfer, *Journal of Computational Physics* (2004).
- [7] A. G. Irvine, I. D. Boyd, N. A. Gentile, Reducing the spatial discretization error of thermal emission in implicit monte carlo simulations, *Journal of Computational and Theoretical Transport* 45 (1-2) (2016) 99–122. arXiv:<https://doi.org/10.1080/23324309.2015.1060245>, doi:10.1080/23324309.2015.1060245.
URL <https://doi.org/10.1080/23324309.2015.1060245>
- [8] C. Ahrens, E. Larsen, A semi-analog monte carlo method for grey radiative transfer problems, in: *Proceedings of the ANS Topical Meeting: International Conference on Mathematical Methods to Nuclear Applications*, 2001.
- [9] M. S. McKinley, E. D. B. III, A. Szoke, Comparison of implicit and symbolic implicit monte carlo line transport with frequency weight vector extension, *Journal of Computational Physics* (2003).
- [10] J.-F. Clouët, G. Samba, Asymptotic diffusion limit of the symbolic monte-carlo method for the transport equation, *Journal of Computational Physics* 195 (1) (2004) 293 – 319. doi:<https://doi.org/10.1016/j.jcp.2003.10.008>.
URL <http://www.sciencedirect.com/science/article/pii/S0021999103005333>
- [11] A. B. Wollaber, E. W. Larsen, On the stability of the ahrens-larsen or smc equations for thermal radiative transfer, in: *Transactions of the American Nuclear Society*, 2010.
- [12] M. A. Cleveland, N. Gentile, Mitigating teleportation error in frequency-dependent hybrid implicit monte carlo diffusion methods, *Journal of Computational and Theoretical Transport* (2014).
- [13] D. Mihalas, B. W. Mihalas, *Foundations of Radiation Hydrodynamics*, Dover Publications, 1999.
- [14] J. Castor, *Radiation hydrodynamics*, Cambridge University Press, 2004.
- [15] G. C. Pomraning, *The equations of radiation hydrodynamics*, Dover Publications, 1973.
- [16] G. Poëtte, CONTRIBUTION TO THE MATHEMATICAL AND NUMERICAL ANALYSIS OF UNCERTAIN SYSTEMS OF CONSERVATION LAWS AND OF THE LINEAR AND NONLINEAR BOLTZMANN EQUATION, Habilitation à diriger des recherches, Université de Bordeaux 1 (Sep. 2019).
URL <https://hal.archives-ouvertes.fr/tel-02288678>
- [17] B. Lapeyre, E. Pardoux, R. Sentis, Méthodes de Monte Carlo pour les équations de transport et de diffusion, no. 29 in *Mathématiques & Applications*, Springer-Verlag, 1998.
- [18] D. Dureau, G. Poëtte, Hybrid Parallel Programming Models for AMR Neutron Monte-Carlo Transport, in: *Joint International Conference on Supercomputing in Nuclear Applications + Monte-Carlo*, no. 04202 in *Parallelism and HPC*, Monte-Carlo, 2013.

- [19] A. Henry, The Application of Reactor Kinetics to the Analysis of Experiments, Nucl. Sci. Engng 3 (1958) 52–70.
- [20] A. Henry, N. Curlee, Verification of a Method for Treating Neutron Space-Time Problems, Nucl. Sci. Engng 4 (1958) 727–744.
- [21] K. Ott, D. Meneley, Accuracy of the Quasistatic Treatment of Spatial Reactor Kinetics, Nucl. Sci. Engng 36(3) (1969) 402–411.
- [22] M. Dahmani, Résolution des équations de la cinétique des réacteurs par la méthode nodale mixte duale utilisant le modèle quasi-statique amélioré et implémentation dans le code CRONOS, PhD thesis, Faculté des Sciences de Rabat, Maroc (1999).
- [23] C. Patricot, Couplages multi-physiques : évaluation des impacts méthodologiques lors de simulations de couplages neutronique/thermique/mécanique., Ph.D. thesis, thèse de doctorat dirigée par Allaire, Grégoire Mathématiques appliquées Paris Saclay 2016 (2016).
URL <http://www.theses.fr/2016SACLX007>
- [24] A. Bernede and G. Poëtte, An Unsplit Monte-Carlo solver for the resolution of the linear Boltzmann equation coupled to (stiff) Bateman equations, Journal of Computational Physics 354 (2018) 211 – 241. doi:<https://doi.org/10.1016/j.jcp.2017.10.027>.
URL <http://www.sciencedirect.com/science/article/pii/S0021999117307805>
- [25] G. Saporta, Probabilités, Analyse de Données et Statistique, 2e édition, Technip, 2006.
- [26] E. Brun, F. Damian, C. Diop, E. Dumonteil, F. Hugot, C. Jouanne, Y. Lee, F. Malvagi, A. Mazzolo, O. Petit, J. Trama, T. Visonneau, A. Zoia, Tripoli-4®, cea, edf and areva reference monte carlo code, Annals of Nuclear Energy 82 (2015) 151 – 160, joint International Conference on Supercomputing in Nuclear Applications and Monte Carlo 2013, SNA + MC 2013. Pluri- and Trans-disciplinarity, Towards New Modeling and Numerical Simulation Paradigms. doi:<https://doi.org/10.1016/j.anucene.2014.07.053>.
URL <http://www.sciencedirect.com/science/article/pii/S0306454914003843>
- [27] D. Hilbert, Begründung der kinetischen gastheorie, Math. Ann. 72 (1912) 562–577.

Appendix A. Short description of the Marshak benchmark of [7]

The test-case corresponds to the study of a 1D Marshak wave [13] with dimensionless units. A black body heats the left boundary of the domain $x \in \mathcal{D} = [0, 4]$ with temperature $T(x = 0) = 1$. The radiation constant is $a = 1$ and so is the speed of light $c = 1$. There is no scattering (i.e. $\sigma_s = 0$) and $\sigma_t(T_m) = \sigma_a(T_m) = \frac{10}{T_m^3}$. Note that this benchmark will demonstrate our new MC solver can be used with temperature dependent opacities. Besides, the test-problem considers a perfect gas eos with $\rho = 1$ and $C_v = 7.14$. The medium is initially cold as $T(x, t = 0) = T_0(x) = 10^{-2} \forall x \in \mathcal{D} = [0, 4]$. We are here interested in the (material and radiative) temperature profiles at $t^* = 500$.

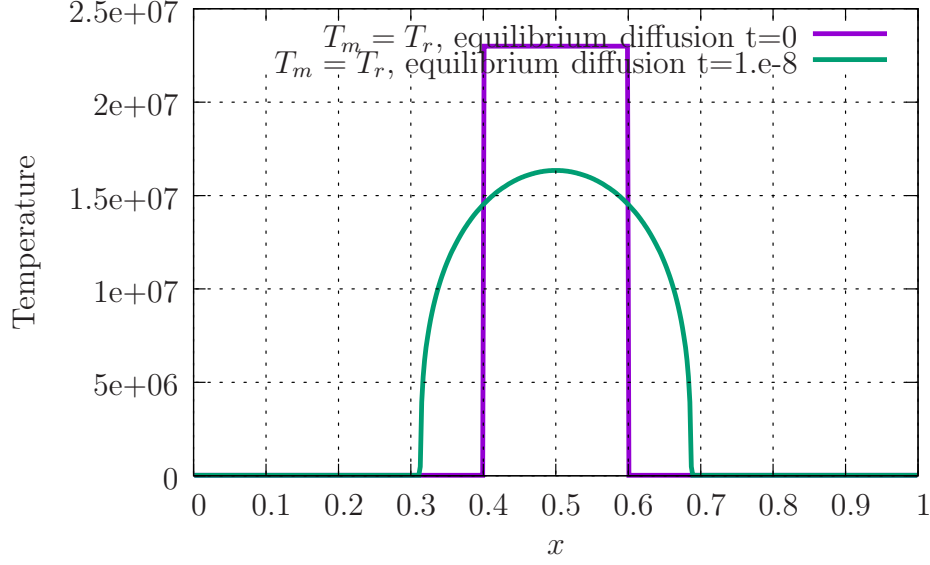


Figure B.6: Initial and final spatial profile of the temperatures ($T_m = T_r$) in the equilibrium diffusion limit for the 'fil rouge' test-problem of this paper.

Appendix B. Details about the second benchmark (see [2])

The initial and boundary conditions together with the problem justifications are provided here for both, the sake of conciseness of the paper and of reproducibility of the results. This second benchmark can be described as follows: let us consider a 1D spatial domain such that $x \in \Omega = [0, 1]$. The domain is filled with a diffusive media $\sigma_t = 2000$, with no (physical) scattering, i.e. $\sigma_s = 0$ and $\sigma_t = \sigma_a$. Initially, temperature of 2.3×10^7 for $x \in [0.4, 0.6]$ and 2.3×10^4 elsewhere. In other words, we have at $t = 0$:

$$T_m(x, t = 0) = T_r(x, t = 0) = 2.3 \times 10^7 \mathbf{1}_{[0.4, 0.6]}(x) + 2.3 \times 10^4 \mathbf{1}_{[0, 1] \setminus [0.4, 0.6]}(x).$$

Note that $\mathbf{1}_\Omega(x)$ denotes the indicatrix of domain Ω . The initial condition is displayed in figure B.6 together with the solution of system (2) at final time $T = 10^{-8}$. This reference solution has been obtained solving (2) with a deterministic solver (with a fine mesh).

Note that for time $t \in [0, T]$, the solution does not reach the boundaries. This test-case has been chosen precisely in order to avoid having to resort to the sampling of boundary particles so that there are no sampled particles for $t > 0$ (as both nssIMC and ISMC avoid source sampling). The radiative constant is set to $a = 10^{-14}$, the speed of light to $c = 3 \times 10^{10}$. A perfect gas is considered so that $E(T_m) = \rho C_v T_m$ with $\rho = 20$, $C_v = 4 \times 10^7$. The configuration may not appear particularly physical but is still relevant for real life encountered difficulties.

Appendix C. Minimal modifications to implement nssIMC into a legacy IMC solver

```

#BEGINNING OF TIME STEP  $[t^n, t^n + \Delta t]$ 
for  $i \in \{1, \dots, N_x\}$  do
    #Compute  $(\Phi^{n,i})_{i \in \{1, \dots, N_x\}}$  from the energy array  $(E^{n,i})_{i \in \{1, \dots, N_x\}}$ 
     $\Phi^{n,i} = \cos(E^{n,i})$ ,  $\beta^{n,i} = \beta(E^{n,i})$ 
    #Update the Fleck factor and the absorption and scattering opacities
     $f^{n,i} = \frac{1}{1 + c\Delta t \sigma_a^{n,i} \beta^{n,i}}$ ,  $\Sigma_a^{n,i} = \sigma_a^{n,i} f^{n,i}$ ,  $\Sigma_s^{n,i} = \sigma_a^{n,i} (1 - f^{n,i}) + \sigma_s^{n,i}$ 
    #keep the density of photon into memory and build the source term
     $U^{0,i} = U^i$ ,  $S^i = c\sigma_a^{n,i} f^{n,i} \Phi^{n,i}$ 
    #Set to zero the (mesh) arrays in which will be tallied the MC particle contributions
     $U^i = 0$ ,  $\Delta E^i = 0$ 
end
#disable source sampling
SourceSampling()
for  $p \in \{1, \dots, N_{MC}\}$  do
    set  $s_p = 0$  #this will be the current time of particle  $p$ 
    # $i_p$  is such that  $\mathbf{1}_{\Omega_{i_p}}(x_p(s_p)) = 1$  (current cell for particle  $p$ )
    while  $s_p < \Delta t$  do
        if  $x_p \notin \mathcal{D}$  then
            | apply_boundary_conditions( $x_p, s_p, \mathbf{v}_p$ )
        end
        #sample the collision time from an uniform sampling  $\mathcal{U}$ 
         $\tau = -\frac{\ln(\mathcal{U})}{c\sigma_t^{n,i_p}}$ 
        if  $\tau > \Delta t$  then
            #move the particle  $p$ , update  $s_p$  to end the treatment of the current particle
             $x_p = x_p + \omega_p \times (t - \tau)$ ,  $s_p \leftarrow t$ 
            #tally the contribution of particle  $p$  in the in which it ends:
             $U^{i_p} += w_p$ 
        end
        else
            #move the particle  $p$ , update the life time of particle  $p$ 
             $x_p \leftarrow x_p - \omega_p \tau$ ,  $s_p \leftarrow s_p + \tau < t$ 
            #keep the old weight into memory
             $w_p^0 = w_p$ 
            #change the particle weight
             $w_p \leftarrow w_p \times \frac{\Sigma_s^{n,i_p}}{\Sigma_t^{n,i_p}}$ 
            
$$w_p \leftarrow w_p \times \left( \frac{\Sigma_s^{n,i_p}}{\Sigma_t^{n,i_p}} + \frac{S^{i_p}}{c\Sigma_t^{n,i_p} \left( U^{0,i_p} e^{-c\Sigma_a^{n,i_p} \tau} + S^{i_p} \frac{1 - e^{-c\Sigma_a^{n,i_p} \tau}}{c\Sigma_a^{n,i_p}} \right)} \right)$$

            #tally (conservatively) the contribution to matter
             $\Delta E^{i_p} += w_p^0 - w_p$ 
            #Sample the angle  $\mathbf{W}'$  of particle  $p$  after the collision from the scattering law
             $\omega_p = W'$ 
        end
    end
end
end

```

Algorithm 1: To implement nssIMC into a legacy IMC code (semi-analog MC scheme), disable source sampling and change the weight modification of the MC particles encountering a collision.